Associated conference: 5th International Small Sample Test Techniques Conference

Conference location: Swansea University, Bay Campus

Conference date: 10th - 12 July 2018

How to cite: Šebek, F., Dymáček, P., Kubík, P., Hůlka, J. & Petruška, J. 2018. The role of punch eccentricity in small punch testing. *Ubiquity Proceedings*, 1(S1): 43 DOI: https://doi.org/10.5334/uproc.43

Published on: 10 September 2018

The role of punch eccentricity in small punch testing

F. Šebek [1,*], P. Dymáček [2], P. Kubík [1], J. Hůlka [3] and J. Petruška [1]

[1] Institute of Solid Mechanics, Mechatronics and Biomechanics, Faculty of Mechanical Engineering, Brno University of Technology, Technická 2896/2, 616 69 Brno, Czech Republic
[2] CEITEC IPM, Institute of Physics of Materials, Academy of Sciences of the Czech Republic, Žižkova 22, 616 62 Brno, Czech Republic
[3] Institute of Applied Mechanics, Resslova 972/3, 602 00 Brno, Czech Republic
***** Correspondence: sebek@fme.vutbr.cz; Tel.: +420 54114 4925

Abstract: The small punch testing technique under quasi-static loading was examined in the view of punch eccentricity role. It might arise especially when the ball is used as the penetrating tool, instead of hemispherical-ended punch. The austenitic stainless steel AISI 316L was chosen to execute several various "large scale" tests in order to calibrate the multi-linear stress–strain relationship along with the ductile fracture criterion KHPS. All the calibration procedure was performed without using the small punch testing. Then, the model was applied to small punch tests to observe the prediction ability when compared to real small punch experiments. Consequently, a numerical study was conducted to see the role of eccentricity in the case of 2 and 2.5 mm ball diameters used as the penetrating tool. The magnitude of eccentricity up to 0.3 mm was numerically tested. The results showed negligible role of eccentricity for 2 mm ball diameter and minor role for 2.5 mm diameter and studied material.

Keywords: pressure vessel; piping steel grade; small sample technique; damage; elastic plastic; finite element method; associated flow rule; time independent plasticity; pressure and Lode dependent fracture criterion; nuclear industry

1. Introduction

The small sample techniques have been evolved since the second half of the twentieth century [1,2] along with the development of more accurate measuring systems, which are capable of assessment of such miniaturized testing. The penetration test has several embodiments: the Small Punch Test (SPT); shear punch test; and disc bend test [3–5]. These have been studied by scanning electron microscopy to reveal the changes in microstructure [6]. This can be advantageously used for examination of transition layers or weldments not only for quasi-static loadings but also for creep [7].

There is a shortage of material usable for testing in energy industry applications such as the turbine rotors or cases, pressure vessels and piping, or various components subjected to radiation in the primary circuit within the nuclear power plants [8]. Those facts open wide possibilities in miniaturized testing.

Analytical equations have been formulated in order to describe the states, which the specimen undergoes. Various approximations have been proposed to correlate the data to the standardized tensile test to obtain the basic mechanical properties, such as the yield stress and ultimate tensile strength [9]. It is crucial to interpret the experimental results correctly. This was reflected in using the numerical simulations to obtain more accurate results along with more assessment possibilities. One of them may be the flow curve of material estimated by the optimization task based on the comparison of experimentally and numerically obtained force–deflection curves [10]. Nevertheless, the computations are still complicated by means of numerous uncertainties represented by the presence of friction, unknown clamping forces [11] or eccentricity effect, which is studied within the present paper. The question of eccentricity may arise especially when using a ball as the penetrating tool instead of well centered punch with hemispherical penetrating end.

2. Materials and Methods

The austenitic stainless steel grade of ASI 316L was chosen because of its wide practical applicability in aggressive environments of petrochemical industry for storage tanks with various contents.

The punch eccentricity effect was numerically studied by means of the finite element method. Abaqus 2017 was employed together with Vectorized User MATerial (VUMAT) subroutine written in Fortran 77 imperative programming language. The VUMAT user subroutine was developed in order to implement the ductile fracture criterion, so the displacement at fracture can be tracked as well.

The stress–strain relationship was estimated on the basis of a standard tensile test. It was realized through the hybrid numerical–experimental approach until the satisfying match between the experimental and computational force–displacement curves was reached. Final multi-linear flow curve is depicted in Figure 1. Additionally, elastic properties were defined through the Young's modulus and Poisson's ratio of 160000 MPa and 0.3, respectively. Physical characteristic needed in explicit computations was the density of 7850 kg·m^{-3}.

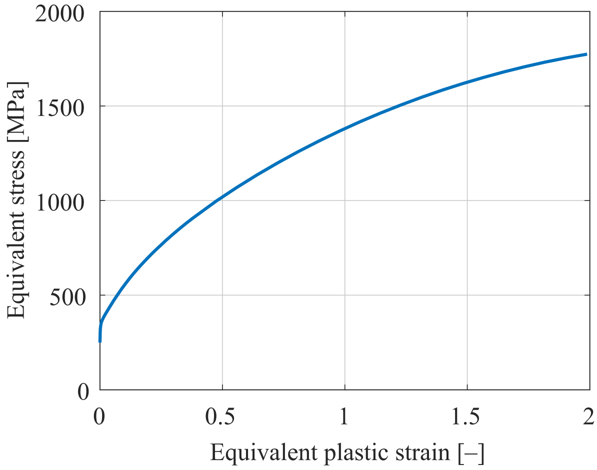

Figure 1. The flow curve in a multi-linear form for AISI 316L.

The ductile fracture was captured by a KHPS criterion with asymmetric weighting function of damage defined as [12]:

$$\bar{\epsilon}^f = \frac{P_5}{\langle \eta - \eta^c \rangle} \xi + \frac{P_4 - P_5}{\langle \eta - \eta^c \rangle} \frac{\xi + 1}{2}, \tag{1}$$

where $\bar{\epsilon}^f$ is the fracture strain, P_4 and P_5 are the material constants, ξ is the normalized third invariant of deviatoric stress tensor, η is the stress triaxiality and η^c is the critical stress triaxiality, which is related to the cut-off region, where there is no damage accumulation because of infinite fracture strain:

$$\eta^c = \left(P_2 - \frac{P_1 - P_3}{2} - P_3 \right) \xi^2 - \frac{P_1 - P_3}{2} \xi - P_2, \tag{2}$$

where P_1, P_2 and P_3 are the material constants of this five parametric failure model.

The damage parameter was tracked through the equivalent plastic strain $\bar{\epsilon}^p$ as:

$$D = \int_0^{\bar{\epsilon}^D} \frac{\mathrm{d}\bar{\epsilon}^p}{\bar{\epsilon}^f}, \tag{3}$$

where $\bar{\epsilon}^D$ is the equivalent plastic strain at fracture for a given loading path at this linear damage accumulation law.

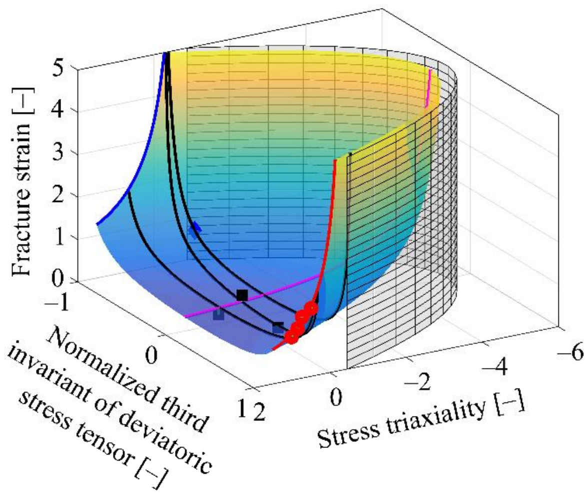

Figure 2. The KHPS criterion calibrated for AISI 316L.

Various fracture tests were used in order to calibrate the model. Those included the tensile tests of smooth and notched cylindrical specimens and notched tubular specimen; tensile–torsional test of notched tubular specimen; torsional test of notched tubular specimen; and compression of notched cylindrical specimen. These eight independent tests are represented by points in Figure 2 along with the calibrated fracture envelope. The state variables cannot be measured directly, so those were obtained from the numerical simulations. The calibration itself was realized through the averaged stress triaxiality and normalized third invariant of deviatoric stress tensor within MATLAB 2016b. All fracture-related material constants are given in Table 1.

Table 1. Material constants of a KHPS criterion for 316L.

P_1 [1]	P_2 [1]	P_3 [1]	P_4 [1]	P_5 [1]
0.471	5.416	0.873	1.583	2.980

3. Results

Real SPTs were performed using the hemispherical-ended punch of 2 mm in diameter. All these experiments should represent the case with no eccentricity. On the other hand, the device can work with a ball, too. The centering may not be ensured well if the ball is used, so the numerical analysis of three eccentricities of 0.1; 0.2; and 0.3 mm was conducted.

Numerical simulations with two widespread ball diameters of 2 mm and 2.5 mm were carried out. The first was directly compared to the experiments (Figure 3a) while the second one only served for observing the influence numerically (Figure 3b). The material behavior was only isotropic homogeneous with associated flow rule obeying von Mises plasticity, which is dependent on the second invariant of deviatoric stress tensor.

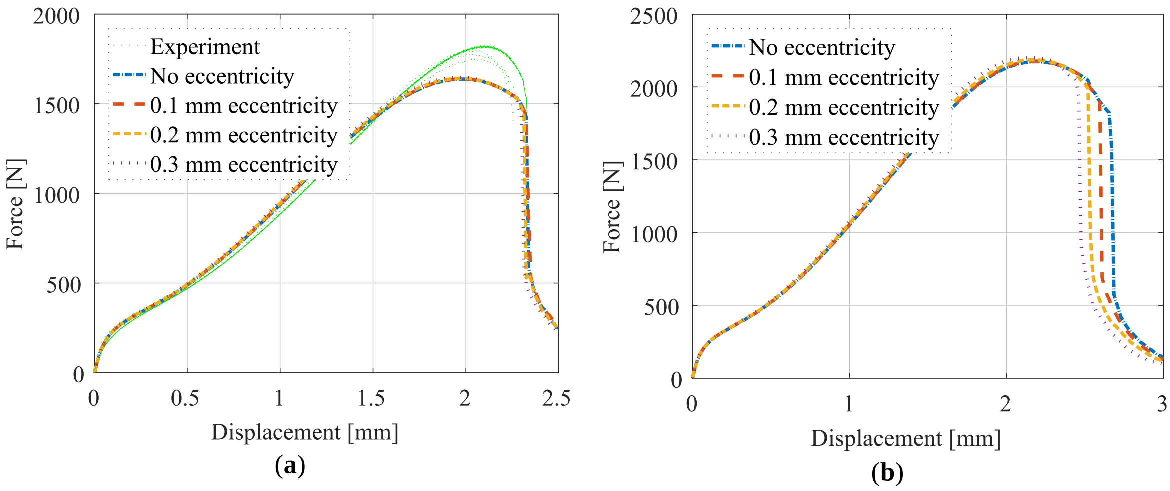

Figure 3. The SPT with punch of: (**a**) 2 mm in diameter within the experiments and numerical simulations; (**b**) 2.5 mm in diameter within the numerical simulations.

4. Discussion

The eccentricity had been assumed to play a negligible role in all previous studies. This was fully confirmed for the austenitic stainless steel and quasi-static SPT with 2 mm ball. For the 2.5 mm ball, the punching force is not influenced, whereas the displacement at fracture is. Both the eccentricity influence and the fit between the experimental and numerical curves of 2mm penetrator could be further improved. It could be interesting to incorporate the approach of continuum damage mechanics [13] because of the non-proportionality of the loading, which may play a role [14]. Another possibility is to use the plasticity model dependent on the normalized third invariant of deviatoric stress tensor [15], or to account for the material anisotropy. It would be useful to conduct a similar analysis for creep as well [16].

5. Conclusions

The small punch test was numerically studied in the view of punch eccentricity for AISI 316L steel grade. It was shown that the presumption of negligible influence of eccentricity is not always justified.

The computations revealed that there is almost no influence for ball of 2 mm in diameter, for which the experiments with some scatter was available. On the other hand, there is an apparent effect of eccentricity on the displacement at fracture for the case of ball of 2.5 mm in diameter. It needs a further study in accounting for more complex material description, which could apply to a broader range of metals.

Acknowledgments: This work is an output of project NETME CENTRE PLUS (LO1202) created with financial support from the Ministry of Education, Youth and Sports under the „National Sustainability Programme I".

References

1. Manahan, M.P.; Argon, A.S.; Harling, O.K. The development of a miniaturized disk bend test for the determination of postirradiation mechanical properties. *J. Nucl. Mater.* **1981**, *103–104*, 1545–1550, DOI: 10.1016/0022-3115(82)90820-0.
1. Lucas, G.E.; Okada, A.; Kiritani, M. Parametric analysis of the disc bend test. *J. Nucl. Mater.* **1986**, *141–143*, 532–535, DOI: 10.1016/S0022-3115(86)80096-4.
2. Kohse, G.; Ames, M.; Harling, O.K. Progress in developing DBTT determinations from miniature disk bend tests. *J. Nucl. Mater.* **1986**, *141–143*, 513–517, DOI: 10.1016/S0022-3115(86)80092-7.
3. Mao, X.; Takahashi, H. Development of a further-miniaturized specimen of 3 mm diameter for TEM disk (ø 3 mm) small punch tests. *J. Nucl. Mater.* **1987**, *150*, 42–52, DOI: 10.1016/0022-3115(87)90092-4.
4. Lucas, G.E. Review of small specimen test techniques for irradiation testing. *Metall. Trans. A* **1990**, *21*, 1105–1119, DOI: 10.1007/BF02698242.
5. Ma, Y.W.; Yoon, K.B. Assessment of tensile strength using small punch test for transversely isotropic aluminum 2024 alloy produced by equal channel angular pressing. *Mater. Sci. Eng. A* **2010**, *527*, 3630–3638, DOI: 10.1016/j.msea.2010.02.057.
6. Rouse, J.P.; Cortellino, F.; Sun, W.; Hyde, T.H.; Shingledecker, J. Small punch creep testing: review on modelling and data interpretation. *Mater. Sci. Technol.* **2013**, *29*, 1328–1345, DOI: 10.1179/1743284713Y.0000000278.
7. Halabuk, D.; Návrat, T. Thermomechanical assessment of fuel rod cladding made of zirconium alloy and silicon carbide material during reactivity-initiated accident. *Nucl. Sci. Eng.* **2018**, *189*, 69–81, DOI: 10.1080/00295639.2017.1373518.
8. Dobeš, F.; Dymáček, P.; Besterci, M. Estimation of the mechanical properties of aluminium and an aluminium composite after equal channel angular pressing by means of the small punch test. *Mater. Sci. Eng. A* **2015**, *626*, 313–321, DOI: 10.1016/j.msea.2014.12.054.
9. Abendroth, M.; Kuna, M. Determination of deformation and failure properties of ductile materials by means of the small punch test and neural networks. *Comput. Mater. Sci.* **2003**, *28*, 633–644, DOI: 10.1016/j.commatsci.2003.08.031.
10. Andrés, D.; Dymáček, P. Study of the upper die clamping conditions in the small punch test. *Theor. Appl. Fract. Mech.* **2016**, *86*, 117–123, DOI: 10.1016/j.tafmec.2016.07.012.
11. Kubík, P.; Šebek, F.; Hůlka, J.; Petruška, J. Calibration of ductile fracture criteria at negative stress triaxiality. *Int. J. Mech. Sci.* **2016**, *108–109*, 90–103, DOI: 10.1016/j.ijmecsci.2016.02.001.
12. Kubík, P.; Šebek, F.; Petruška, J. Ductile fracture criteria in prediction of slant fracture. In ECCOMAS Congress 2016, Proceedings of the 7th European Congress on Computational Methods in Applied Sciences and Engineering, Crete, Greece, 5–10 June 2016; Papadrakakis, M., Papadopoulos, V., Stefanou, G., Plevris, V., Eds.; Institute of Structural Analysis and Antiseismic Research School of Civil Engineering, National Technical University of Athens (NTUA): Athens, Greece; CS 212; 6699–6710.
13. Šebek, F.; Petruška, J.; Kubík, P. The role of loading path in ductile fracture. In Insights and Innovations in Structural Engineering, Mechanics and Computation, Proceedings of the 6th International Conference on Structural Engineering, Mechanics and Computation, Cape Town, South Africa, 5–7 September 2016; Zingoni, A., Ed.; Taylor & Francis Group: London, Great Britain; 090; 550–556.
14. Šebek, F.; Petruška, J.; Kubík, P. Behavior of Lode dependent plasticity at plane strain condition and its implication to ductile fracture. *Solid State Phenom.* **2017**, *258*, 213–216, DOI: 10.4028/www.scientific.net/SSP.258.213.
15. Dobeš, F.; Dymáček, P. Fracture-based correlation of uniaxial and small punch creep data. *Theor. Appl. Fract. Mech.* **2016**, *86*, 34–38, DOI: 10.1016/j.tafmec.2016.08.020.